Chemical and ecotoxicological assessment of poly(amidoamine) dendrimers in the aquatic environment

I.J. Suarez, R. Rosal, A. Rodriguez, A. Ucles, A.R. Fernandez-Alba, M.D. Hernando, E. García-Calvo

Poly(amidoamine) (PAMAM) dendrimers are attracting great interest as a consequence of their unique properties as carriers of active molecules in aqueous media, as we expect their presence in the environment to be widespread in the future.

In this article, we focus on the analytical methods to characterize and to determine these polymeric materials in waters and on their ecotoxicity for aquatic organisms. We review physical characterization techniques (e.g., light scattering, electron microscopy, atomic force microscopy) and analytical techniques, mainly based on liquid chromatography, so as to consider their main capabilities, advantages and drawbacks. We assessed the toxicity of certain PAMAM dendrimers for the green alga *Pseudokirchneriella subcapitata* by determining the EC_{50} and correlating it with the ζ-potential.

Keywords: Aqueous environment; Atomic force microscopy; Dendrimer; Ecotoxicity; EC_{50}; Electron microscopy; Light scattering; Liquid chromatography; Poly(amidoamine); ζ-potential

I.J. Suarez, R. Rosal, A. Rodriguez
Department of Chemical Engineering, University of Alcalá, 28771 Alcalá de Henares, Spain

A. Ucles, A.R. Fernandez-Alba*
Centro de Investigaciones de la Energía Solar (CIESOL), Department of Hydrogeology and Analytical Chemistry, University of Almería, 04120 La Cañada de San Urbano, Almería, Spain

M.D. Hernando
National Reference Centre for Persistent Organic Pollutants, University of Alcalá, 28871 Alcalá de Henares, Madrid, Spain

E. García-Calvo, A.R. Fernandez-Alba
Fundación IMDEA-Agua, C/ Punto Net 4, 2ª planta, Edificio ZYE, Parque Científico Tecnológico de la Universidad de Alcalá. 28805, Alcalá de Henares, Madrid, Spain

*Corresponding author.
Tel.: +34 950 015 034;
Fax: +34 950 015 483;
E-mail: amadeo@ual.es

1. Introduction

Dendrimers are a new class of polymeric materials, generally described as macromolecules and characterized by an extensively branched 3D structure providing a high degree of surface functionality and versatility. The unique properties associated with dendrimers (e.g., uniform size, high degree of branching, water solubility, multivalency, defined molecular weight and available internal cavities) make them attractive for biological and drug-delivery applications.

Dendrimers are perfectly branched building block polymers that emerge radially from a central core [1]. The poly(amidoamine) (PAMAM) dendrimers have diameters of 1.5–13.5 nm, so they can be viewed by direct techniques {e.g., electron microscopy [2–6], atomic force microscopy (AFM) [3,7,8]} or indirect techniques {e.g., light scattering [9–12]}.

Structurally, the dendrimer comprises three fundamentals parts:

0165-9936/$ - see front matter © 2011 Elsevier Ltd. All rights reserved. doi:10.1016/j.trac.2010.11.009

(1) the core;
(2) the dendrons; and,
(3) the terminal groups.

The core must have reactive centres to which the dendrons (branches) are attached. Fig. 1 shows the cores more commonly used. The dendron has terminal groups that become the new centre of support. Each completed dendron layer around the core is called a generation, the first layer being generation zero. Generation n is usually denoted as Gn, where G is generation, and n is the number of layers. Dendrimers obtained in an intermediate step, before completing layer n + 1, are denoted Gn.5. The extension .5 is refers to intermediate syntheses (or half generation) [13]. The assembly of dendrons is usually carried out in two steps, using a Michael addition synthesis [14]. The first report of these kinds of molecules was made by Vögtle et al. [15], who described a series of synthetic cascade molecules (see references in Vögle's book [1].

In the case in this work, when dendrons are amide-amine structures, the dendrimer is PAMAM. Tomalia reported the first work and took out the first patent on PAMAM dendrimers, with both ammoniac and ethylendiamine cores, some of the most used in research [13,16,17]. Fig. 2 represents the synthesis and divergence of PAMAM, as reported by Tomalia [13], and shows an example of third-generation PAMAM. These PAMAM dendrimers generally have $–NH_2$, –OH, –COOH, $–COOCH_3$ terminal groups located on the external layer, and, in all cases, they have tertiary nitrogens in the inner structure, positioned on the branching points [18]. In general, with respect to PAMAM dendrimers, when the name of the terminal group is not specified, the intention is that the PAMAM referred too has $–NH_2$ as the terminal group. As a consequence, these dendrimers have two pKa corresponding to the terminal group and the tertiary amine {i.e. 9.52 and 6.30, respectively, in the case of PAMAM [19–21]}. At neutral pH, most of the primary amines are protonated, and, at pH < 4, all of the tertiary amines are also protonated, as reported by van Duijvenbode et al. [22]. Similar results with PAMAM dendrimers were also reported by Diallo et al. [23,24].

The branched structures of dendrimers have been studied from a fractal point of view [25–27]. Farin found that PAMAM dendrimers have a fractal dimension of 2.4, similar to enzymes, and suggested that these materials can act as biomolecular mimics with important physiological interactions [26].

PAMAM dendrimers can be used as:
(1) additives in the pharmaceutical and cosmetic industries;
(2) drug carriers (molecular vector) [28–30];
(3) analytical sensors [31–33] because one of the main reasons for the interest in PAMAM dendrimers is their capability in trapping specific molecules thus faciliting their water solubility [13,16];
(4) a chelating agent of metals for remediation of wastewater [23,24]; and,
(5) a carrier of Pt metal in hydrogenation catalysts [34].

PAMAM dendrimers of high generations (above generation 4) have structures that exhibit densely packed near-spherical topologies with many nm-sized cavities [35] (e.g., which can act as organic molecule reservoirs or nanoscale templates to produce metal nanoparticles (NPs) [36–39].

Because we expect PAMAM dendrimers to have widespread future use in human consumption, and then be waste after release to environment, our main objective in this work is to review and to show results on the characterization and the analysis of PAMAM dendrimers in aqueous media and their effect on ecotoxicity.

2. Characterization in the aquatic environment

In aqueous media, PAMAM dendrimers with functional groups (-NH_2, -OH, -COOH) are very soluble [20,23]. Table 1 shows the amounts of water bound inside PAMAM at different pH levels and generations: in some cases the molar ratio of water:dendrimers is between 138 (generation 4, high pH) and 1731 (generation 6, low pH), as reported by Maiti et al. [20].

For the same generation of PAMAM dendrimer, the bound water increases when the pH decreases due to an increased protonation level in which the tertiary amines are protonated together to the primary amine on the shell, facilitating penetration of water inside the particle. Also, at a higher generation, the amount of water increases due to the increase in sites that can be bound.

When a non-polar solvent (e.g., acetonitrile) is used instead, the PAMAM dendrimer aggregates

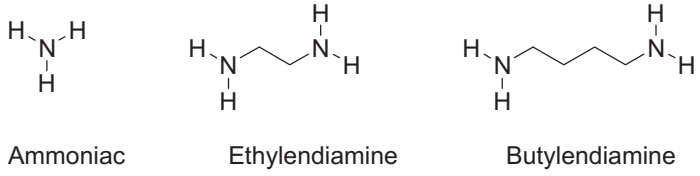

Figure 1. Examples of several types of PAMAM core.

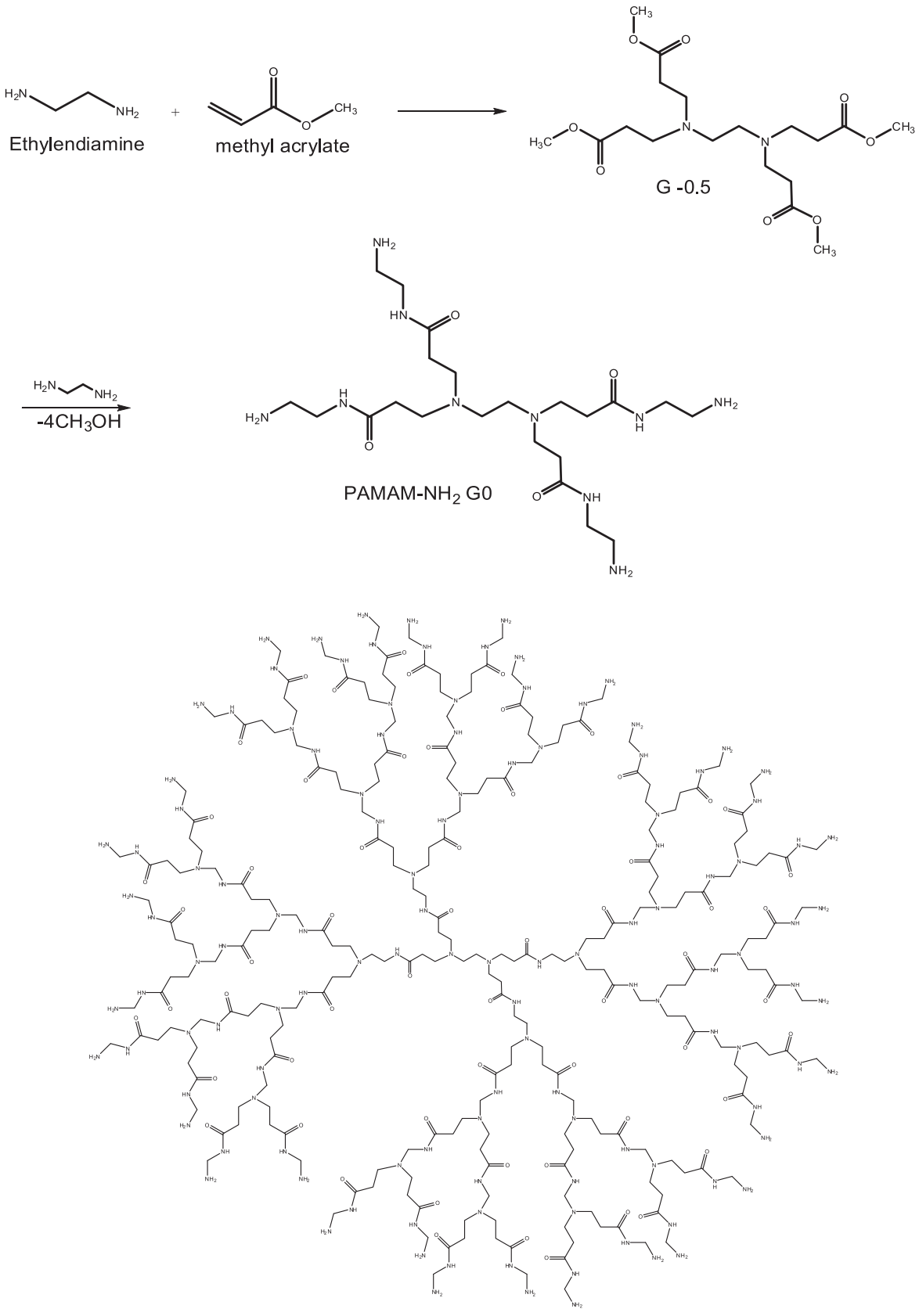

Figure 2. (Top) Divergent synthesis of G0.0 PAMAM, according to Tomalia et al. [13]. (Bottom) G3 PAMAM.

Table 1. Average amount of water inside dendrimer at various pH levels for different generations of PAMAM dendrimers [20]

Generation	pH > 12	pH ~ 7	pH < 4
4	138	201	325
5	378	524	757
6	890	1344	1731

[12,20,40,41]. For this, it is important to note that the dendrimer–solvent interaction depends on the natures of the functional groups located on the periphery of the dendrimers and the solvent used. Hyydrogen-bond interactions are therefore frequently found in hydrophilic dendrimers. By tuning these properties, we can obtain aggregation phenomena or dendrimer solubilization.

The number of terminal functional groups increases exponentially with the number of the generation. This also depends both on the core and the dendrons. In the case of PAMAM with an ethylene-diamine core, the number of functional groups on the periphery of the particle increases in geometric progression to the number of the generation [42]. If the terminals groups are $–NH_2$ or –OH, the pH should substantially affect the surface-charge density of the particles. The level of protonation is calculated [Equation (1)] using the Henderson-Hasselbach equation [24,43,44]:

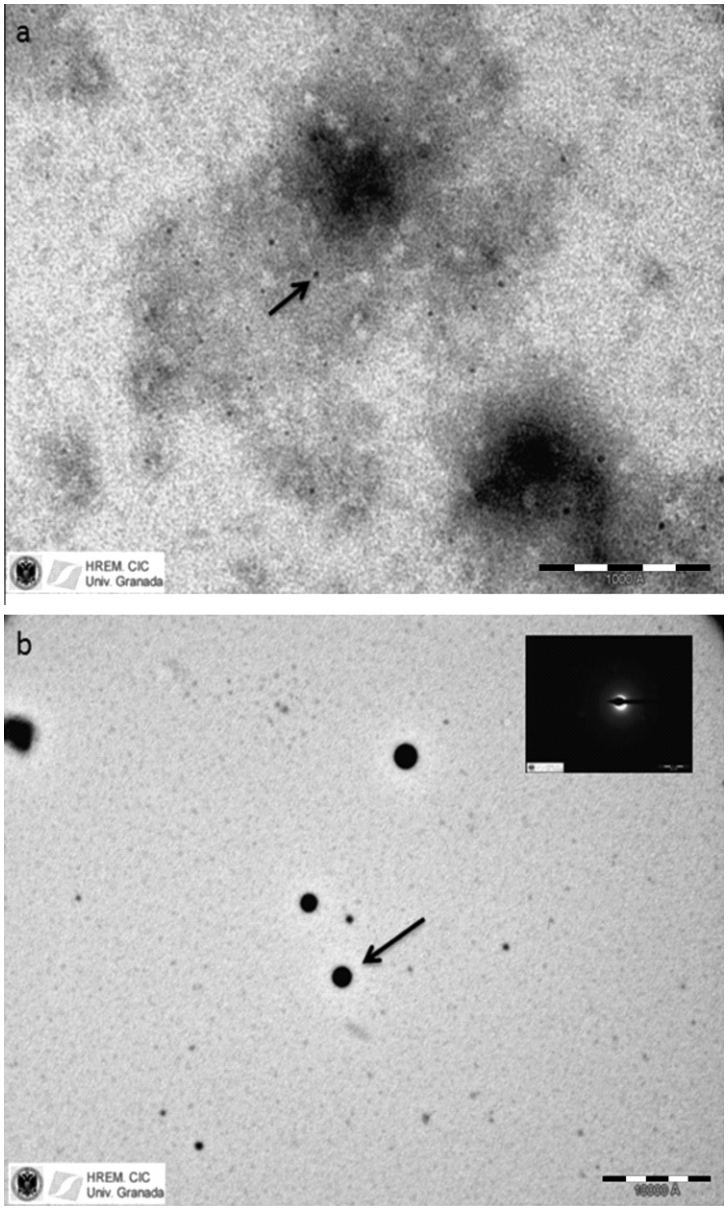

Figure 3. (a) High-resolution transmission electron microscopy (HRTEM) of G4 PAMAM; the sizes are of the order of 5 nm in diameter. Bar reference is 100 nm. (b) HRTEM of adduct PAMAM-NH_2(G4)-SDS at pH 7; the sizes are of the order of 200 nm in diameter (cf. Fig. 6). Bar reference is 1000 nm. Inset reveals with X-ray diffraction that particles have no order. The arrows show examples of PAMAM particles present on each sample.

$$log\frac{\alpha}{1-\alpha} = pKa - pH \quad (1)$$

where α is the level of protonation. At neutral pH, an α value of 0.99 has been reported. This means that almost all the groups, whether $–NH_2$ or –OH, are protonated (i.e. these particles maintain a positive charge in aqueous solution, and ternary nitrogen has α values of 0.17–0.41; and, at a pH below 3, all nitrogens (primary and tertiary) are 100% protonated [23]. This magnitude would have a remarkable influence on electrokinetic properties (e.g., electrokinetic mobility, and zeta potential), and then on stability in the dispersion. The aggregation of PAMAM can be influenced by the interaction from these positively-charged particles with anionic surfactants, which are negatively charged {e.g., sodium dodecyl sulfate (SDS) [45]} that can be present in the aquatic environment. In this, it will form an adduct with the dendrimer, whose external layer will be the alkyl side (hydrophobic) of this surfactant. In this region, aggregation will take place due to the van der Waals interactions.

3. Characterization by instrumental techniques

The instrumental methods most frequently used are:
(1) nuclear magnetic resonance (NMR) [46,47];
(2) X-ray crystal structure analysis on the hybrid dendrimer with metallic oxide [4];
(3) small-angle neutron scattering (SANS) [48];
(4) light scattering [12,49,50];
(5) scanning probe microscopy [51–54];
(6) transmission electron microscopy (TEM) [2];
(7) chromatography with its variants – liquid chromatography (LC), preparative LC, gel permeation chromatography [55], and gel electrophoresis [56]; and,
(8) mass spectrometry (MS).

Some of these techniques can help us to understand the interaction between dendrimers and solvents or electrolytes. With TEM especially, it is possible to image dendrimers. This is a valuable method for studying the size and the stability of PAMAM dendrimers [2]. Due to the lower atomic number of the atoms that constitute the dendrimer scaffold, the contrast is weaker; the dendrimers are stained, adding atoms rich in electrons. In the case of PAMAM, it is stained with an aqueous solution of sodium phosphotungstate as a contrast agent [2]. However, there are other contrast agents (e.g., uranyl acetate and osmium tetroxide) [57].

We performed assays with high-resolution TEM (HRTEM) for the adduct PAMAM-NH_3^+ with anionic surfactant sodium docecyl sulfate (SDS) and with the original PAMAM G4 at neutral pH. Fig. 3 shows the results, and we can see how a larger particle is formed due to supramolecular assembly [45]. In the inset of Fig. 3b, X-ray probe diffraction reveals a disordered or glassy structure on this assembly, which agrees with the glass-transition temperature of 282 K for the PAMAM G4 dendrimer [58].

In contrast to TEM, in which the image is bidimensional (2D), AFM gives us 3D information about the particle. AFM involves scanning a tip probe on the surface, using a servo-mechanical device that detects the force field generated between the tip and the sample, as well as the change in distance between the tip and the surface. In this way, it is possible to draw the 3D features of the object with atomic resolution. The principles of AFM have been described [59,60]. The information obtained with PAMAM reveals the importance of the substrate on which the particle is supported. These interactions can be:
(1) electrostatic, in the case of mica substrate, which is negatively-charged and interacts with the positively-charged PAMAM dendrimer [61]; or,
(2) covalent, as is the case with Au, forming an Au-N bond [62].

These interactions, producing the flattening of the PAMAM dendrimers [63], lead to underestimation of the height and to overestimation of the diameter of such dendrimers. Compared to other substrates, PAMAM experiences lower interaction energy, producing less flattening with respect to mica [64].

We have used light scattering, electron microscopy, chromatographic and MS techniques for supporting and comparing the data obtained by other authors.

4. Characterization by light-scattering techniques

Light scattering is a result of the interaction (generally elastic) between the electromagnetic wave and matter. This interaction causes a deviation in the path of the radiation coming from the light source. The sources of electromagnetic waves are generally He-Ne or Ar lasers, X-ray radiation, electrons or neutrons. Although the scattering mechanism is different in each case, the basic element that unites and is ultimately so important in the study of soft matter is the concept of interference and its relation to the structure of the soft-matter medium [65]. Electron scattering refers to electron microscopy (scanning or transmission mode) yielding a topographic image that reveals the inner structure of the particles [66,67].

The scattering is detected outside the sample as a function of the scattering angle. In general, the amplitude of the scattered wave at a given time depends on the interference between waves scattered by the different scattering centres in the scattering medium. An important quantity in scattering experiment is the scattering vector $\vec{q}$, defined as $\vec{q} = \vec{kl} - \vec{kf}$, where $\vec{kl}$ is the propagation vector, and $\vec{kf}$ the scattered vector. The magnitude of $\vec{q}$ is given by:

$$q = \frac{4\pi}{\lambda} sin\left(\frac{\theta}{2}\right)$$

where λ is the wavelength of the incident beam, assuming it is similar to wavelength of the scattered beam (elastic interaction), and θ is the angle between $\vec{kl}$ and $\vec{kf}$. In terms of particles, it may be interpreted,, when q is multiplied by $h/2\pi$ (Planck's constant divided by 2π), as the momentum transfered to the system by the photons [65]. In a dispersion, in which there is a collection of particles of several, or similar, sizes, the incoming beam hits them. As particles undergo Brownian motion, the scattered signal experiences both constructive and destructive interference, and this is recorded by an array of photomultipliers that are analyzed over time and the data are then compared using correlation functions. At the start times, the signal are similar, and the normalized correlation function is near to 1. This function becomes decorrelated at later times, decreasing exponentially to reach a constant value. This decrease is correlated with the translational diffusion coefficient of the particles. The scattered radiation gives us information about the shape and the structure of the material. This information can be obtained by tuning the scattering vector $\vec{q}$ (changing the scattering angle, or wavelength of incident beam). This modulation can be made while recording the intensity of scattering, with either the angle of dispersion, or measuring the function of correlation at different angles. The first case is known as ''static light scattering'', and the second known as ''dynamic light scattering'' (DLS).

We are interested in the DLS technique [68], because it is possible to calculate the size of the particle. The quantity calculated is the translational diffusion coefficient, D, and, assuming a spherical geometry, by using the Stoke-Einstein relation, Equation (2), we can calculate the radius of particles:

$$D = \frac{kT}{6\pi\eta a} \tag{2}$$

where a is the radius of the particle, η is the solvent viscosity, T is absolute temperature and k is the Boltzman constant.

In mathematical terms, the intensity of scattering, as a function of the magnitude of scattering vector (q), gives information on the arrangement and the spacing of the polymer segment. In Fig. 4, Bauer shows the existence of voids in the PAMAM-dendrimer structure [69]. The solid line represents the evolution of size with molecular weight when considering a completely collapsed structure; the voids are present due to the real size being greater than that of this collapsed structure. In Fig. 5, Prosa et al. show, by using small-angle X-ray scattering (SAXS), the dependence of q on the generation of the PAMAM dendrimer, and give us the evolution of the structure when the shape goes from star to sphere [70].

The drawback of using this technique on a PAMAM dendrimer is that it has a refractive index similar to the

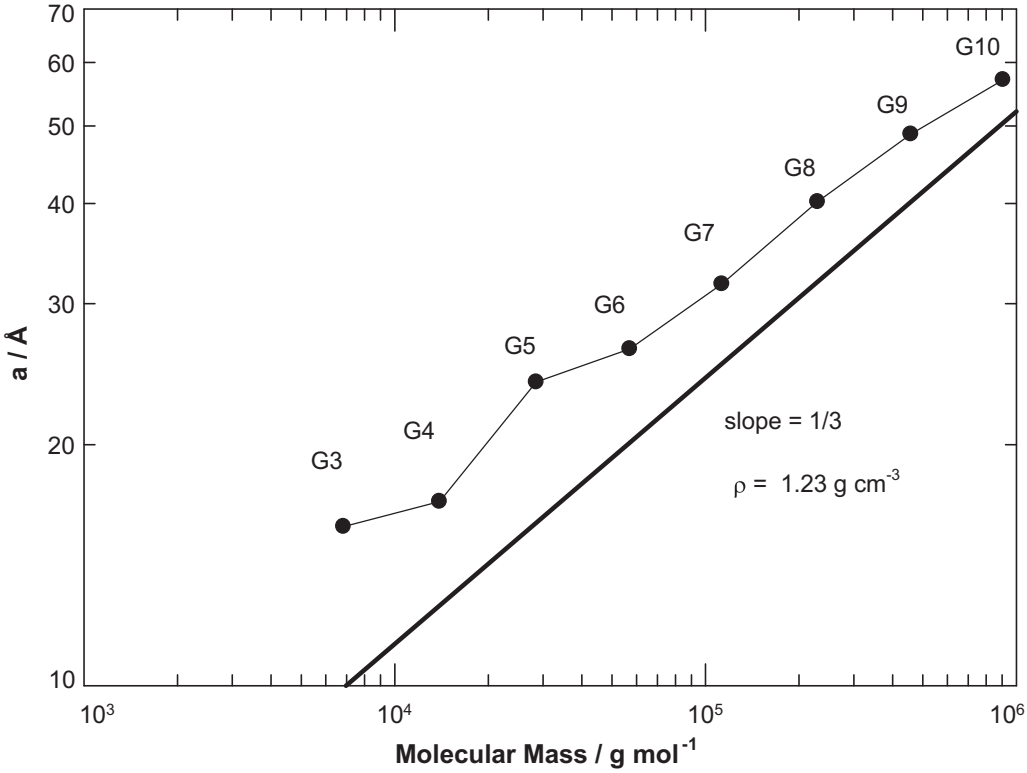

Figure 4. Radius, a, of PAMAM dendrimers at several generation numbers, G3–G10, calculated by SAXS. The straight line is the limit of PAMAM dendrimers collapsed to bulk density. The 1/3 power law suggests uniform spherical shape. The theoretical radius, a, of spheres with a density of 1.23 g/cm^3, based on the value reported for PAMAM [69].

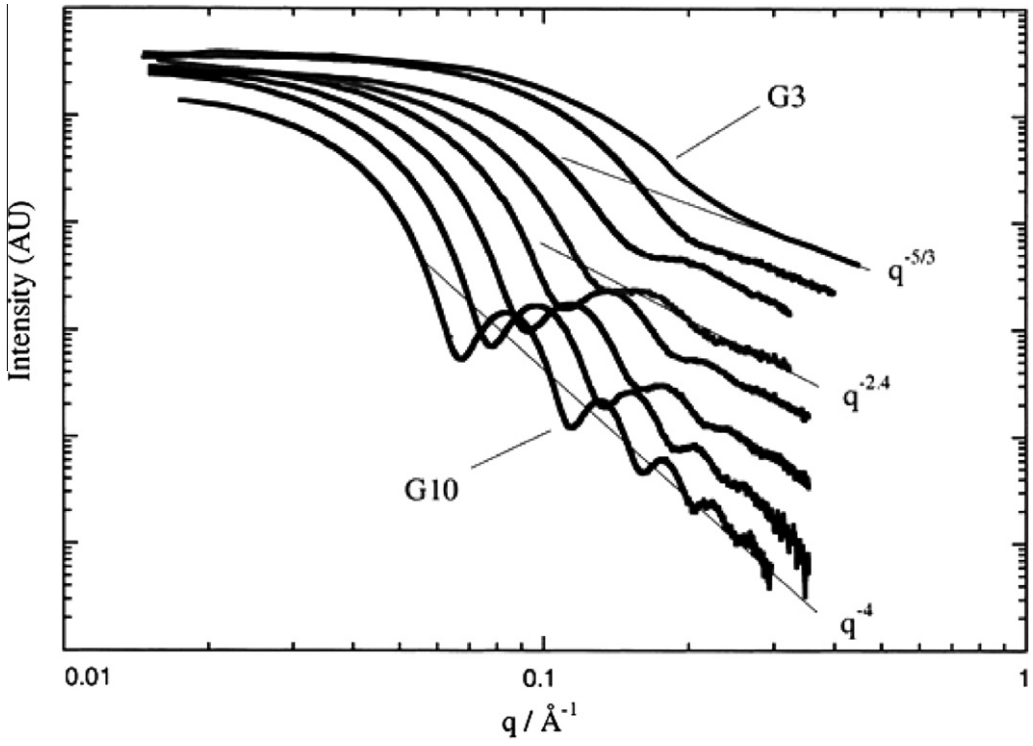

Figure 5. SAXS curves for PAMAM mass fraction 1% dendrimer/methanol solutions of generation G3 (top) through G10 (bottom). The progression of secondary features and limiting power-law behavior suggest an evolving intramolecular organization (Reprinted with permission from [70]).

dispersant media (water). For this reason, the intensity of scattering is very low, making it difficult to obtain a consistent size measurement at an angle of scattering above 100° [68]. This problem was overcome by Orberg et al. [50] using angles of scattering below 100° and with a high concentration of PAMAM particles (of the order of 18 mg/mL). They reported size measurements of G4 PAMAM dendrimers in aqueous media. These were carried out using equipment with a variable angle using a goniometer with an Nd:YAG solid-state laser-diode light source of wavlength 532 nm. These measurements closely agreed with the size stated by the manufacturer (i.e. 4.5 nm diameter at a scattering angle of 90°).

As PAMAM can be present in different wastewater environments, we used an aqueous solution of an amphipathic molecule as a model for soaps. We chose SDS as an agent that aggregates, followed by an increase of the particle size, and modifies its refractive index. This

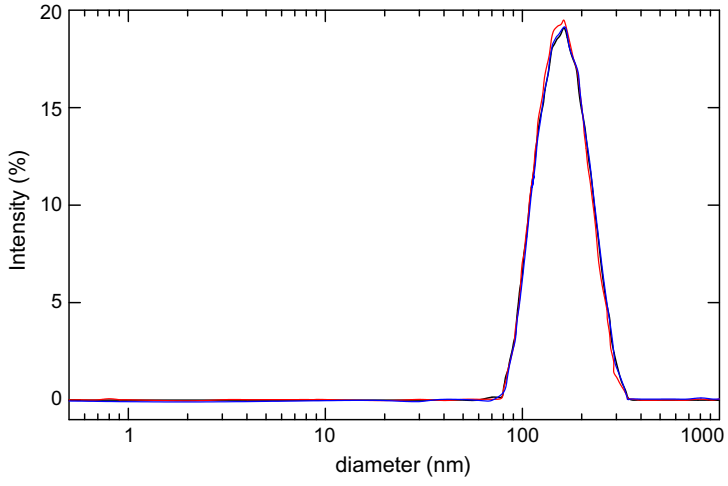

Figure 6. Size-distribution graph obtained for the G4 PAMAM dendrimer at 0.2 mM at neutral pH with SDS at 5 mM. Three measurements of the same solution were performed. The average size was 154.1 nm (±1.1 nm).

increase in size can be monitored using DLS and TEM. We employed the method described by Wang et al. for preparing the dendrimer solutions with SDS [45]. In Fig. 6, we show the size distribution of the PAMAM-NH_2-SDS adduct. Comparing this with Fig. 3b, in which the same dispersion was used for imaging by TEM, we found that the particles matched in size using both techniques.

Regarding the effect of pH on the structure, Liu et al. [48] resolved the controversy between theoretical and experimental results, using simulations of molecular dynamics. Their conclusion is that there were small changes in the size but that there was an internal restructuring caused by a pH-induced conformational change from a ''dense core'' (high pH) to a ''dense shell'' (low pH). They suggested how PAMAM dendrimers might be used as drug-delivery vehicles, as encapsulation and release of guest molecules could be controlled using pH as the trigger.

5. Chromatographic techniques

Several coupled detectors [e.g., UV, refractive index, multiangle laser light scattering (MALLS) and MS] have been used to evaluate generations of PAMAM dendrimers [55,71,72].

MALLS detectors comprise a detector array pre-fixed at several angles that simultaneously measure the scattered-signal intensity at each of the angles to give information about molecular mass and particle size [73].

LC columns have been used to separate and to characterize PAMAM dendrimers [55]. In many cases, these chromatographic methods have also been appropiate for separating PAMAM dendrimers when the surface-amine groups were substituted for other groups (e.g., hydroxyl, acetyl or carboxyl), and where structural differences between generations of dendrimers were present [74].

Size-exclusion chromatography (SEC) [or gel-permeation chromatography (GPC)] columns have also been used to separate different generations of PAMAM dendrimers based on molecular weight [55]. SEC with a MALLS detector is the most reliable method to determine average molar mass of dendrimers, because no calibration standards are needed, and this is the ideal technique for the characterization of different generations because there are many structural differences between generations of PAMAM dendrimers.

In addition, SEC can be used for detecting generational impurities (e.g., dimers, oligomers and supramolecular aggregates) that can appear in the synthesis of dendrimers. SEC columns have also provided good separation efficiency and good sensitivity [limit of detection (LOD), 2 mg/mL]. Some disadvantages include possible interactions of the solute with the solid phase or the limited size-separation range of the columns, which may not cover the size range of both primary NPs and their aggregates [75].

LC and GPC techniques have been applied to characterize poly(propylenimine) (POPAM) dendrimers of different generations [75]. These have been analyzed by SEC with gel-filtration columns to determine molecular weights. The mobile phase used was an acidic buffer solution. LC measurements were then made with an acidic solution as the eluent in a gradient-mode analysis and a C-18 reversed-phase column. The retention time for hybrid dendrimers (G2:G4, G3:G4, and G4:G4) was 35 min, 36 min and 37 min, respectively, indicating poor separation between the different generations of dendrimers. However, Cason et al. [74] proposed the use of LC to separate various dendrimers. They evaluated G4 and G5 PAMAM dendrimers with a C18 column. The mobile phase was water [acidified with trifluoroacetic acid (TFA)] and acetonitrile [also acidified with TFA] in gradient mode. The retention time of the G4 and G5 PAMAM dendrimers was 6.90 min and 7.1 min, respectively, indicating similar problems in the separation of dendrimers. Results showed enhancement in retention time as a function of PAMAM generation, due to the geometrically-increased surface density of the terminal-amine groups and TFA-ion pairs. Also observed was the presence of a peak at 7.41 min, generated by the impurities associated with using TFA [69].

In another way, Shi et al.[76] employed G1–G5 PAMAM dendrimers, the surfaces of which were converted to acetyl groups (Gn-Ac). SEC columns were used to separate different generations of dendrimers with an acidic buffer solution as the mobile phase. Also, a C5 RP-HPLC column was used to separate dendrimers. This comprised water (acidified with TFA) and acetonitrile (acidified with TFA) in gradient mode. The retention times for the dendrimers were 15.09 min (G1-Ac), 17.95 min (G2-Ac), 19.80 min (G3-Ac), 21.32 min (G4-Ac) and 22.66 min (G5-Ac). These results showed little separation between the different generations of dendrimers.

Islam also used ethylenediamine-core G5 PAMAM dendrimers and a C5 silica-based LC column. The mobile phase for elution of PAMAM dendrimer comprised water and acetonitrile (both acidified with TFA) in a gradient mode. The retention time was 14 min for the G5-NH_2 dendrimer. Besides the main peak, two smaller peaks could also be identified and attributed to the structural defects present during synthesis of the dendrimer [77].

We have performed chromatographic analysis of G0–G3 dendrimer samples (PAMAM-dendrimer kit) with ethylenediamine cores in methanol solution. All dendrimer samples were then dried and redissolved in the HPLC mobile phase, which comprised water with 0.1% formic acid. We performed LC separations with two coupled LC columns, an SEC column of 250 mm × 4.6 mm and 4-μm particle size and a reversed-phase C5 column of 250 mm × 4.6 mm and 5-μm particle size. The mobile phase for elution of PAMAM dendrimer derivatives of different generations was an isocratic mode comprising water with 0.1% formic acid. All the samples were dissolved in the aqueous mobile phase (water containing 0.1% formic acid) at 1 mg/mL concentration. The detection of eluted

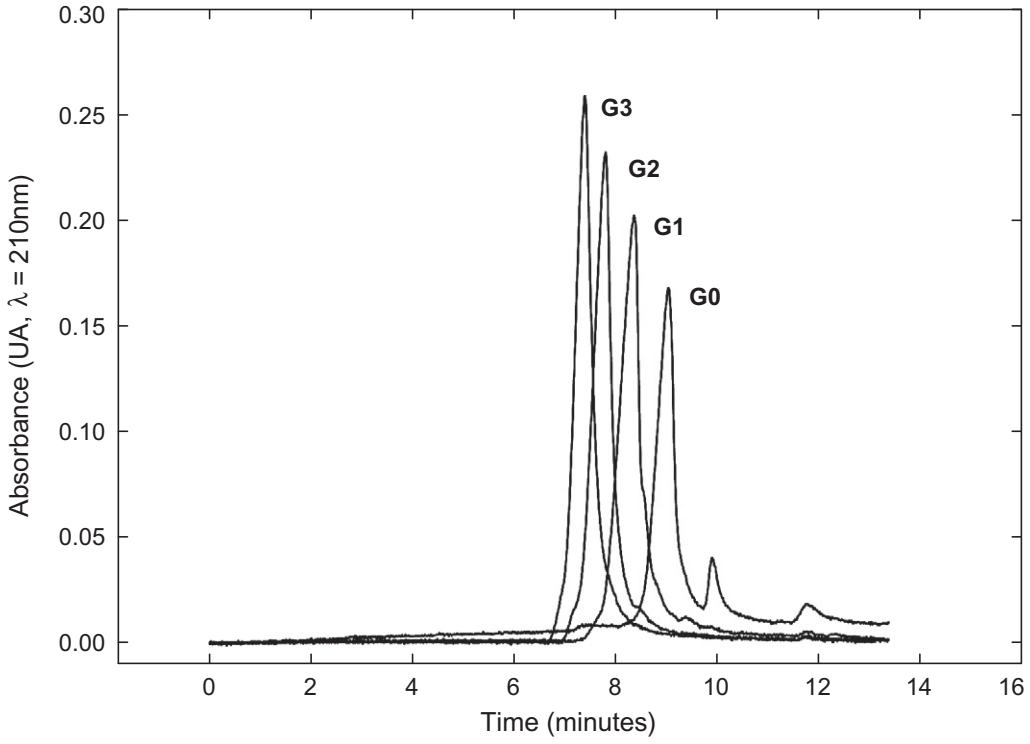

Figure 7. HPLC chromatograms of amine-terminated PAMAM dendrimers of different generations injected separately. Isocratic mode comprised water with 0.1% formic acid. Injection: 20 μL.

samples was performed at 210 nm and the injection volume was 20 μL. Fig. 7 shows the results, with the chromatograms of G0 through to G3 amine-terminated dendrimers (G0–G3). In the chomatogram, we can see how the retention time increases with decreasing dendrimer generation. The retention times for the PAMAM dendrimers were 9.05 min (G0), 8.38 min (G1), 7.80 min (G2) and 7.39 min (G3). As we can see, the advantage of using two coupled LC columns is that, within a single analysis, we were able to separate the different generations of PAMAM dendrimers successfully. We also calculated the LOD of the G0 PAMAM dendrimer to be 100 mg/L.

Other analytical techniques [e.g., MS with laser desorption and electrospray ionization (ESI)] have been used to evaluate PAMAM dendrimers. The advantage of MS methods [e.g., matrix-assisted laser desorption/ionization (MALDI)] is that they can be used for the structural characterization of various fractions isolated with the help of a previous chromatographic purification.

In contrast to Subbi et al. [71], we used an LC-time-of-flight (TOF)-MS system to evaluate PAMAM dendrimers. The main advantage of this method was its high sensitivity and selectivity. We focused on the fragmentation process itself and on the fragments that were formed in the course of ESI in positive-ion mode.

LC separations were performed with two coupled LC columns, an SEC column of 250 mm × 4.6 mm and 4 μm particle size and a C5 column of 250 mm × 4.6 mm and 5 μm particle size. Some 20 μL of sample extract was injected in each run. The mobile phase for elution of PAMAM-dendrimer derivatives of different generations was an isocratic mode comprising water with 0.1% formic acid. All the samples were dissolved in the aqueous mobile phase (water containing 0.1% formic acid) at a concentration of 1 mg/mL.

Our fragmentation analysis mainly concentrated on G0, which, because of its mass (517 Da), was in the most convenient mass region for detailed MS analysis. Fig. 8 shows the TOF mass spectra of the G0 PAMAM dendrimer. An abundant protonated G0-NH_2 molecule was observed as an intense peak at m/z 517.3915 in the mass spectra, together with the sodium adducts detected at m/z 539.3780, respectively. We can also see a signal at m/z 403.3129, which might be associated with the loss of an amidoamine group in the G0 PAMAM dendrimer molecule.

We calculated the LOD of the G0 PAMAM in water to be 10 mg/L.

Other non-chromatographic methods (e.g., MALDI-TOF-MS) have been used [78], because of their advantages (e.g., high molecular-weight range, sensitivity, and mass accuracy). However, the main disadvantage is the search for an optimal matrix and a proper sample-preparation method for a given analyte.

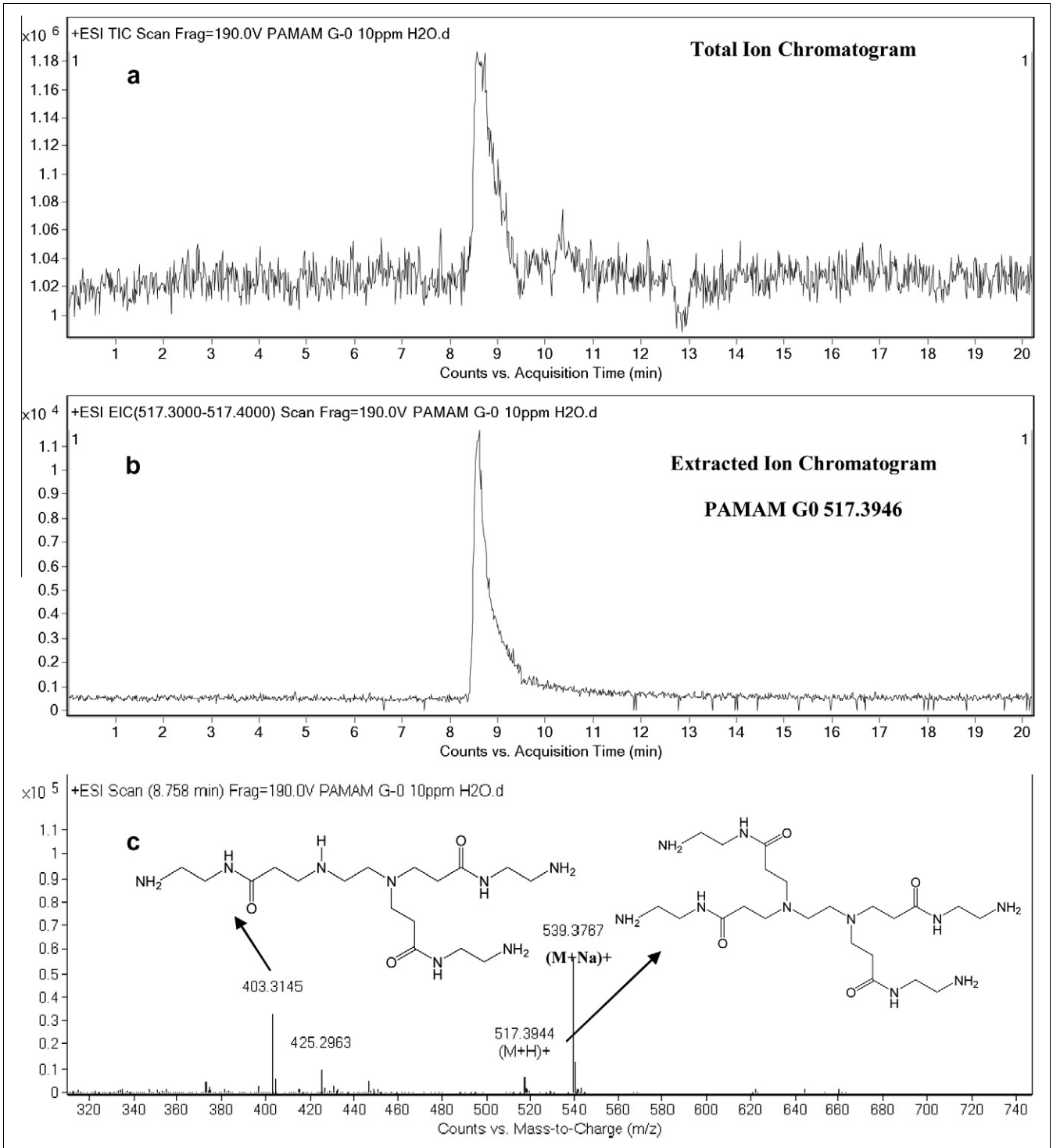

Figure 8. (a) Total ion chromatogram of a G0 PAMAM sample. (b) Extracted ion chromatogram for the exact mass of G0 PAMAM. (c) Mass spectrum of the extracted peak.

6. Field-flow fractionation (FFF)

Field-flow fractionation (FFF) is a promising technique for the size separation of NPs (e.g., dendrimers) in complex natural samples [72].

The advantages of FFF include minimal exposure of the dendrimers to surfaces during separation because there is no stationary phase, particularly compared to SEC, and the ability to adjust the system to different particle-size ranges by changing the perpendicular field [71]. An

Table 2. Retention times for different generations of PAMAM dendrimers using AsFlFF technique at pH 10.2 and 3.1 [72]

Generation	Retention time (min) (pH = 10.2)	Retention time (min) (pH = 3.1)
4	4.66	1.45
5	6.14	2.04
6	8.26	2.92
7	10.18	4.25
8	13.36	5.76
9	17.87	8.14

important issue in FFF is obtaining clean separations of different-sized components [78]. FFF can also be coupled to a range of sensitive, multi-element techniques (e.g., MALLS) and inductively coupled plasma (ICP)-MS [79]. The limitations of FFF techniques are:

(1) membrane or accumulation wall interactions;
(2) continuous reequilibration in the channel and the need for preconcentration;
(3) additional concentration of the sample during equilibration and an increased possibility of aggregation in the channel; and,
(4) sensitivity.

Asymmetrical flow FFF (AsFlFFF) was tested by Lee et al. [72] as an alternative to the chromatographic techniques for the separation of G4.0–G9.0 PAMAM dendrimers. To minimize interactions with the membrane, careful optimization of experimental conditions (e.g., flow rate and pH) may be required. AsFlFFF could

Table 3. Techniques frequently used to evaluate PAMAM dendrimers

Technique	PAMAM dendrimer	Column	ID	LOD	Ref.
LC-UV	G1–G6	C5, C18	λ = 210 nm	100 mg/L	[55,76,77,80]
LC-MS (TOF)	G0–G3	SEC coupled C5	$[M+H]^+$ $[M-115]^+$	10 mg/L	[81]
FFF-RI	G4–G9	—		—	[72]
MALDI-TOF-MS	G2–G10	—	$[M+H]^+$	—	[71,82,83]

ID, Identification; LOD, limit of detection.

Table 4. Summary of ecotoxicity data reported for PAMAM dendrimers

PAMAM generation and core	Surface groups	Test models	EC_{50}-IC_{50} (μM)*	Ref.
G4 ethylenediamine core	NH_2	*Danio rerio* embryos (24 h)**	1.0 (0.9–1.2)	[85]
		Danio rerio embryos (72 h)**	0.6 (0.5–0.6)	
		Danio rerio embryos (120 h)**	0.4 (0.3–0.4)	
G2 ethylenediamine core	NH_2	*Vibrio fischeri* (30 min)	194 (66–321)	[86]
G5 ethylenediamine core	NH_2	*Vibrio fischeri* (30 min)	27 (14–40)	[86]
G4 ethylenediamine core	NH_2	*Vibrio fischeri* (5 min)	16.30	[87]
		Vibrio fischeri (15 min)	6.17	
		Vibrio fischeri (30 min)	3.11	
		Daphnia magna (24 h)	1.13	
		Daphnia magna (48 h)	0.68	
		Thamnocephalus platyurus (24 h)	2.90	
G5 ethylenediamine core	NH_2	*Vibrio fischeri* (5 min)	15.18	[87]
		Vibrio fischeri (15 min)	5.08	
		Vibrio fischeri (30 min)	1.64	
		Daphnia magna (24 h)	0.72	
		Daphnia magna (48 h)	0.27	
		Thamnocephalus platyurus (24 h)	1.81	
G6 ethylenediamine core	NH_2	*Vibrio fischeri* (5 min)	4.80	[87]
		Vibrio fischeri (15 min)	1.64	
		Vibrio fischeri (30 min)	0.83	
		Daphnia magna (24 h)	0.32	
		Daphnia magna (48 h)	0.13	
		Thamnocephalus platyurus (24 h)	1.11	
G2 1,4-diaminobutane core	NH_2	*Chlamydomonas reinhardtii* (72 h)	0.590 (0.548–0.630)	[88]
G4 1,4-diaminobutane core	NH_2	*Chlamydomonas reinhardtii* (72 h)	0.208 (0.180–0.237)	[88]
G5 1,4-diaminobutane core	NH_2	*Chlamydomonas reinhardtii* (72 h)	0.167 (0.158–0.171)	[88]

*95% confidence intervals when available.
**Continuous exposure post fertilization.

be used at acidic, neutral, and even at basic pH for separation and characterization of PAMAM dendrimers. Table 2 shows the retention times obtained for the G4.0–G9.0 PAMAM dendrimers at pH 3.1 and 10.2. It is noticeable that the retention times of the dendrimers increase as the pH and the generation number increase, due to the increase in the hydrodynamic size caused by aggregation of PAMAM particles. The separation between different generations is better when PAMAM particles are neutral (basic pH). Smaller peaks eluting before and after the main peak were found, suggesting small impurities formed during the synthesis of PAMAM dendrimers. AsFlFFF may be coupled with other on-line characterization techniques (e.g., MALLS or a differential viscometer) for more detailed physical characterization of each size fraction separated by AsFlFFF. Table 3 shows different analytical methods used to evaluate PAMAM dendrimers [55,71,72,76,77,80–83].

7. Ecotoxicity

Dendrimers belong to a class of macromolecular therapeutics that includes other particulate drug-delivery systems (e.g., polymeric micelles and liposomes). Even if biomedical dendrimers are still at the early stage of their development, the clinical experience with more classical polymer-derived therapeutics can be used as a guide for dendritic nanomedicine [84]. As indicated before, there are clear data showing that dendrimers can display cytotoxicity, but very limited information is available on their effect on non-target organisms, and, to date, only a few studies have been performed to assess the ecotoxicity of dendrimers as engineered NPs (Table 4).

So far, the most complete study on aquatic organisms was performed by Naha et al. using three polyamidoamine dendrimers (G4–G6) [87]. They demonstrated a significant toxicity that increased with increasing dendrimer generation with median effect values in the range 0.13 μM (7.4 mg/L, *Daphnia magna*, 48 h, G6) to 16.30 μM (231.5 mg/L, *Vibrio fischeri*, 5 min, G4). They also found that the measured EC_{50} values correlated linearly with the observed change in ζ-potential when dendrimers were put in the corresponding assay media [87]. The authors interpreted this result as indicative of the degree of interaction of dendrimers with the medium components that may shield surface charges.

The absence of PAMAM toxicity to *V. fischeri* was also reported by Mortimer et al., who obtained 30 min EC_{50} values of 194 μM (631 mg/L, G2) and 27 μM (775 mg/L, G5) [86], which are in relative agreement with those obtained by Naha et al. [87]. In contrast with these findings, *V. fischeri* was quite sensitive to other carbon-based NPs. Naha et al. reported 5 min EC_{50} of 40.5 mg/L and 25.7 mg/L for N-isopropylacrylamide-co-N-tert-butylacrylamide (NIPAM/BAM) in 65:35 and 50:50 copolymers, respectively [89].

Petit et al. investigated the toxicity of G2, G4 and G5 PAMAM dendrimers on the green alga *Chlamydomonas reinhardtii* [88]. Using cell viability measured from esterase activity as the endpoint, they found that the toxicity expressed in molar concentration increased with dendrimer generation number (0.590 μM, 1.94 mg/L for G2, 0.208 μM, 2.97 mg/L for G4 and 0.167 μM, 4.82 mg/L for G5). This result was similar to that observed by Naha et al. with increasing PAMAM generation [87]. Petit et al. also obtained a stimulatory effect of G2 and G4 on the photosynthetic activity and total chlorophyll content of the green alga, probably because of activation of the photosynthetic electron transport of Photosystem II [88].

Toxicity towards a higher trophic level organism was studied only by Heiden et al., who used zebrafish embryos to assess the developmental toxicity of G3.5 and G4 PAMAM dendrimers, as well as dendrimers bioconjugated with selective ligands (RGD) [85]. They found that G4 dendrimers were toxic towards the growth and the development of the zebrafish embryos, but G3.5 dendrimers, with carboxylic-acid terminal functional groups, did not exhibit toxicity at concentrations as high as 200 μM (average molecular weight 12,931). PAMAM dendrimers with RGD reduced their cytotoxicity with respect to unmodified G4.

Mukherjee et al. showed that the adsorption of proteins on the dendrimer surface resulted in a dramatic change in zeta potential [90]. The connection between toxicity and the physicochemical properties of NPs is still poorly understood and requires further work.

Other aspects are also pending [e.g., internalization, or not, of NPs by cells, and differentiation between true toxic effects and artifacts (e.g., nutrient depletion)]. A great deal of research needs to be conducted to elucidate the underlying mechanism of toxic response, including nanogenotoxicity. Moreover, other dendrimers, apart from PAMAM, must also be tested for ecosystem exposure in tandem with the expected market increase of these nanomaterials.

In this work, the toxicity of G4 and G1 PAMAM dendrimers having an ethylenediamime core was assessed by inhibiting the growth of *Pseudokirchneriella subcapitata*. G4 and G1 PAMAM were manufactured by Dendritech and purchased from Sigma-Aldrich. G4-NH_2, and G1-NH_2, with 64 and 8 surface amino groups, have average molecular weights of 14,214.17 and 1429.85, respectively, and G4-OH contains 64 surface-hydroxyl groups and its molecular weight is 14,277.19.

Zeta potential was measured via electrophoretic light scattering combined with phase-analysis light scattering in the same instrument, equipped with a Malvern autotitrator MPT-2. The measurements were conducted at 25°C using 10 mM in KCl as the dispersing medium and at a concentration of 2 μM (G4) and 20 μM (G1).

The green alga, *P. subcapitata*, was tested using algal-growth inhibition OECD TG 201 (open system) in

96-well microplates culturing the algae in a total volume of 210 μL. Algae beads and culture media were purchased from Microbiotest Inc. Microplates were maintained at 22°C in a growing chamber with controlled light intensity (~100 μE/m^2/s) and humidity levels, without any evaporation of the culture media and with periodic agitation and aeration. The growth of *P. subcapitata* was monitored over 72 h by determining the increase of chlorophyll concentration measured by fluorescence (excitation at 444 nm – emission at 680 nm) using a Fluoroskan Ascent Microplate Fluorometer. At least three replicates of each toxic concentration or blank were assayed with $ZnSO_4$ as the standard for reproducibility control. Dose-effect relationship parameters and their respective confidence intervals were determined using a linear interpolation method that did not assume any particular dose-effect model (USEPA, 2002) [91].

Table 5 lists the results for the growth inhibition of *P. subcapitata*. The toxicity was particularly high for G4-NH_2 with EC_{50} about one quarter of the median effect value compared with that of the lower generation, G1-NH_2. Fig 9 shows full dose-response relationships. This result agrees with the finding of Naha et al. [87], who reported that the toxicity towards different test organisms increased with increasing dendrimer generation, most probably as a consequence of a larger surface area for interaction with living organisms.

ζ-potential values, also listed in Table 4, show relatively high positive values for G4-NH_2. This positive charge is relevant because algal-cell membranes possess large negatively-charged domains, which should favour particle-cell interaction. The toxicity of the negatively-charged, hydroxyl-terminated G4 dendrimer was much lower, with EC_{50} > 40 (growth inhibition at 40 mg/L, 52 ± 6 %). We also used EC_{10} as a surrogate for the no observed effect concentration (NOEC), which showed a clear effect at very low concentrations (i.e. at the hundreds of ppb level for both G4 dendrimers) [92].

At present, environmental risk assessment of nanomaterials is seriously hampered as there is insufficient information, or lack of the essential pieces of information, for the development of the key steps of risk assessment:
(1) hazard identification;
(2) hazard characterization;
(3) exposure assessment; and,
(4) risk characterization.

The features of nanomaterials set new challenges and research needs in developing a suitable risk-assessment framework. In this context, the characterization of test nanomaterials is critical for appropriate hazard and exposure evaluation. It is crucial to ascertain the fate

Table 5. Dose-effect relationship parameters of PAMAM dendrimers for the growth inhibition of *Pseudokirchneriella subcapitata*. EC_{50} and EC_{10} are the doses required to inhibit growth 50% and 10%, respectively

Dendrimer	EC_{50}		EC_{10}		ζ-potential (mV)
	mg/L (nM)	CI 95%	mg/L	CI 95%	
G4-NH_2	1.41 (99)	1.33–1.51 (96–106)	0.21 (15)	0.18–0.25 (13–18)	+26.1 ± 1.6
G4-OH	>40 (>2800)	–	0.43 (30)	0.24–1.88 (17–132)	−1.23 ± 0.40
G1-NH_2	5.86 (4100)	5.44–6.25 (3800–4370)	1.10 (770)	0.67–1.85 (470–1290)	−0.89 ± 0.23

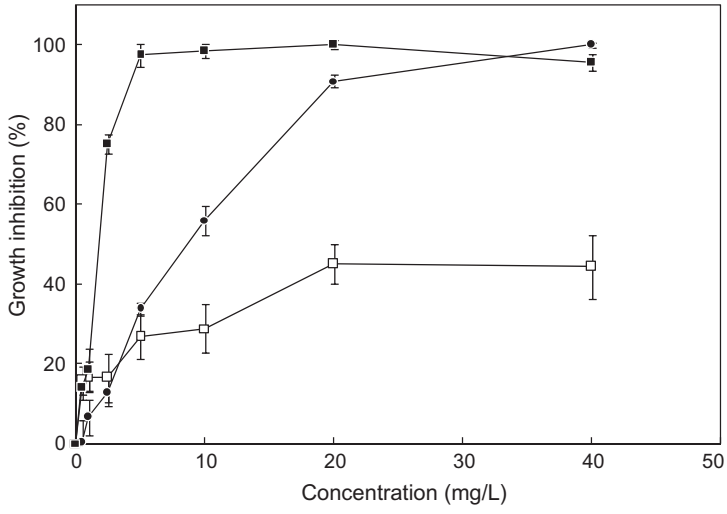

Figure 9. Dose–response for the growth inhibition of *Pseudokirchneriella subcapitata* after 72 h exposed to PAMAM dendrimers G4-NH_2 (■), G1-NH_2 (●) and G4-OH (□).

of nanomaterials considering, among other related parameters, degradation processes and generation of transformation products. In exposure assessment, advances are rare and depend on new developments in analytical methods to detect environmental concentrations. To a great extent, the estimation of environmental concentrations is blocked by the lack of knowledge about the rates of release of nanomaterials to the environment and theories that can help us predict concentrations from release rates.

8. Conclusions

PAMAM dendrimers have great potential for use as carriers of organic molecules in aqueous media, so their characterization and evaluation are of great interest.

Size characterization of PAMAM dendrimers can be performed, preferably by light-scattering techniques (e.g., DLS), but there are difficulties as a consequence of the low intensity of scattering when their concentration is not very high. TEM can also be used to verify the size, the aggregation and the crystalline states of the PAMAM particles. Other techniques (e.g., AFM) are also interesting.

Identification and quantification of PAMAM in environmental waters can be performed by reversed-phase chromatographic techniques coupled to UV or MS detectors. A C5 packaging material is a good column choice, and combination of SEC with C5 columns is more effective. LODs can be as low as 10 mg/L in the case of MS detectors with ESI, but a serious limitation can be the high molecular weights of PAMAM of generations greater than 1 (above 2000 uma).

Other techniques (e.g., FFF) can also be efficient, avoiding transformation processes as a consequence of exposure to the column surface.

Few studies have been performed to assess the ecotoxicity of PAMAM dendrimers. In general, their toxicity increases as the generation increases, but the use of different target organisms and endpoints, as well as the interaction of NPs with other medium components may lead to different conclusions.

Acknowledgements

The authors wish to acknowledge the Spanish Ministry of Science and Innovation for their economic support. A. Uclés acknowledges the research fellowship from the Spanish Ministry of Science and Innovation associated with the NANOAQUAL project (Ref. CTM2008-04239).

References

[1] F. Vögtle, G. Richardt, N. Werner, Dendrimer Chemistry, Wiley-VCH Verlag GmbH & Co. KGaA, Weinheim, Germany, 2009.
[2] C.L. Jackson, H.D. Chanzy, F.P. Booy, B.J. Drake, D.A. Tomalia, B.J. Bauer, E.J. Amis, Macromolecules 31 (1998) 6259.
[3] M.S. Bakshi, A. Kaura, R. Sood, G. Kaur, T. Yoshimura, K. Torigoe, K. Esumi, Colloids Surf., A 266 (2005) 181.
[4] S.L. Sewell, R.D. Rutledge, D.W. Wright, Dalton Trans. 29 (2008) 3857.
[5] M.F. Ottaviani, P. Matteini, M. Brustolon, N.J. Turro, S. Jockusch, D.A. Tomalia, J. Phys. Chem. B 102 (1998) 6029.
[6] W. Zhang, G. Dong, H. Yang, J. Sun, J. Zhou, J. Wang, Colloids Surf., A 348 (2009) 45.
[7] K.-H. Jung, H.-K. Shin, Y.-S. Kwon, C. Kim, Colloids Surf., A 257–258 (2005) 191.
[8] E. Balnois, K.J. Wilkinson, Colloids Surf., A 207 (2002) 229.
[9] J.L. Barrat, J.F. Joanny, P. Pincus, J. Phys. II 2 (1992) 1531.
[10] K. Esumi, K. Kuwabara, T. Chiba, F. Kobayashi, H. Mizutani, K. Torigoe, Colloids Surf., A 197 (2002) 141.
[11] M.M. Haridas, J.R. Bellare, Colloids Surf., A 133 (1998) 165.
[12] M.J. Jasmine, M. Kavitha, E. Prasad, J. Lumin. 129 (2009) 506.
[13] D.A. Tomalia, H. Baker, J. Dewald, M. Hall, G. Kallos, S. Martin, J. Roeck, J. Ryder, P. Smith, Polym. J. 17 (1985) 117.
[14] B.D. Mather, K. Viswanathan, K.M. Miller, T.E. Long, Prog. Polym. Sci. 31 (2006) 487.
[15] E. Buhleier, W. Wehner, F. Vögtle, Synthesis (1978) 155.
[16] D.A. Tomalia, J.R. Dewald, U.S. Patent US4507466, 1983.
[17] D.A. Tomalia, H. Baker, J. Dewald, M. Hall, G. Kallos, S. Martin, J. Roeck, J. Ryder, P. Smith, Macromolecules 19 (1986) 2466.
[18] R. Esfand, D.A. Tomalia, Laboratory synthesis of poly(amidoamine) (PAMAM) dendrimers, in: J.M.J. Fréchet, D.A. Tomalia (Editors), Dendrimers and Other Dendritic Polymers, John Wiley & Son, Chichester, West Sussex, UK, 2001, p. 587.
[19] D. Cakara, J. Kleimann, M. Borkovec, Macromolecules 36 (2003) 4201.
[20] P.K. Maiti, T. Cağın, S.-T. Lin, W.A. Goddard, Macromolecules 38 (2005) 979.
[21] Y. Niu, L. Sun, R.M. Crooks, Macromolecules 36 (2003) 5725.
[22] R.C. van Duijvenbode, M. Borkovec, G.J.M. Koper, Polymer 39 (1998) 2657.
[23] M.S. Diallo, W. Arasho, J.H. Johnson, W.A. Goddard, Environ. Sci. Technol. 42 (2008) 1572.
[24] M.S. Diallo, S. Christie, P. Swaminathan, L. Balogh, X. Shi, W. Um, C. Papelis, W.A. Goddard, J.H. Johnson, Langmuir 20 (2004) 2640.
[25] S.M. Aharoni, Polym. Adv. Technol. 6 (1995) 373.
[26] D. Farin, D. Avnir, Angew. Chem., Int. Ed. Engl. 30 (1991) 1379.
[27] D.A. Tomalia, A.M. Naylor, W.A. Goddard III, Angew. Chem., Int. Ed. Engl. 29 (1990) 138.
[28] I.J. Majoros, J.R. Baker, Dendrimer-Based Nanomedicine, Pan Stanford Publishing, Singapore, 2008.
[29] I.J. Majoros, C.R. Williams, J.R. Baker, Curr. Top. Med. Chem. 8 (2008) 1165.
[30] M. Labieniec, C. Watala, Cent. Eur. J. Bio. 4 (2009) 434.
[31] D. Deriu, G. Favero, A. D'Annibale, F. Mazzei, ECS Trans. 16 (2008) 105.
[32] D.-M. Kim, H.-B. Noh, J.S. Koo, Y.-B. Shim, ECS Meeting Abstracts 802 (2008) 2821.
[33] Y. Qu, Q. Sun, F. Xiao, G. Shi, L. Jin, Bioelectrochemistry 77 (2010) 139.
[34] N.N. Hoover, B.J. Auten, B.D. Chandler, J. Phys. Chem. B 110 (2006) 8606.
[35] A.M. Naylor, W.A. Goddard, G.E. Kiefer, D.A. Tomalia, J. Am. Chem. Soc. 111 (1989) 2339.
[36] A.W. Jensen, B.S. Maru, X. Zhang, D.K. Mohanty, B.D. Fahlman, D.R. Swanson, D.A. Tomalia, Nano Lett. 5 (2005) 1171.
[37] M.Q. Zhao, L. Sun, R.M. Crooks, J. Am. Chem. Soc. 120 (1998) 4877.
[38] M.F. Ottaviani, R. Valluzzi, L. Balogh, Macromolecules 35 (2002) 5105.
[39] H. Tokuhisa, M. Zhao, L.A. Baker, V.T. Phan, D.L. Dermody, M.E. Garcia, R.F. Peez, R.M. Crooks, T.M. Mayer, J. Am. Chem. Soc. 120 (1998) 4492.

[40] P.K. Maiti, W.A. Goddard, J. Phys. Chem. B 110 (2006) 25628.
[41] S.H. Kim, J.A. Katzenellenbogen, Angew. Chem., Int. Ed. Engl. 45 (2006) 7243.
[42] D.A. Tomalia, Prog. Polym. Sci. 30 (2005) 294.
[43] V.A. Kabanov, A.B. Zezin, V.B. Rogacheva, Z.G. Gulyaeva, M.F. Zansochova, J.G.H. Joosten, J. Brackman, Macromolecules 31 (1998) 5142.
[44] M. Nagasawa, Pure Appl. Chem. 26 (1971) 519.
[45] C. Wang, E. Wyn-Jones, J. Sidhu, K.C. Tam, Langmuir 23 (2007) 1635.
[46] Y.H. Zhang, T.P. Thomas, A. Desai, H. Zong, P.R. Leroueil, I.J. Majoros, J.R. Baker, Bioconjugate Chem. 21 (2010) 489.
[47] A.D. Meltzer, D.A. Tirrell, A.A. Jones, P.T. Engelfield, D.M. Downing, D.A. Tomalia, Abstracts Papers Am. Chem. Soc. 197 (1989) 38.
[48] Y. Liu, V.S. Bryantsev, M.S. Diallo, W.A. Goddard III, J. Am. Chem. Soc. 131 (2009) 2798.
[49] M.L. Ainalem, A.M. Carnerup, J. Janiak, V. Alfredsson, T. Nylander, K. Schillen, Soft Matter 5 (2009) 2310.
[50] M.-L. Orberg, K. Schillen, T. Nylander, Biomacromolecules 8 (2007) 1557.
[51] W. Wang, W. Xiong, Y.H. Zhu, H.B. Xu, X.L. Yang, J. Biomed. Mater. Res., Part B 93 (2010) 59.
[52] J.-W. Kim, E.-A. Choi, S.-M. Park, J. Electrochem. Soc. 150 (2003) E202.
[53] C.V. Kelly, M.G. Liroff, L.D. Triplett, P.R. Leroueil, D.G. Mullen, J.M. Wallace, S. Meshinchi, J.R. Baker, B.G. Orr, M.M.B. Holl, ACS Nano 3 (2009) 1886.
[54] J. Li, D. Qin, J.R. Baker Jr., D.A. Tomalia, Macromol. Symp. 167 (2001) 257.
[55] M.T. Islam, X. Shi, L. Balogh, J.R. Baker, Anal. Chem. 77 (2005) 2063.
[56] A. Sharma, D.K. Mohanty, A. Desai, R. Ali, Electrophoresis 24 (2003) 2733.
[57] D.B. Williams, C.B. Carter, The Transmission Electron Microscope, Second Edition., Springer US, New York, USA, 2009.
[58] P.R. Dvornic, D.A. Tomalia, Poly(amidoamine) dendrimers, in: J.E. Mark (Editor), Polymer Data Handbook, Oxford University Press, Inc., New York, USA, 1999, p. 266.
[59] P. Samori, J. Mat. Chem. 14 (2004) 1353.
[60] Y. Gan, Surf. Sci. Rep. 64 (2009) 99.
[61] R. Pericet-Camara, G. Papastavrou, M. Borkovec, Langmuir 20 (2004) 3264.
[62] A. Hierlemann, J.K. Campbell, L.A. Baker, R.M. Crooks, A.J. Ricco, J. Am. Chem. Soc. 120 (1998) 5323.
[63] T.A. Betley, M.M. Banaszak Holl, B.G. Orr, D.R. Swanson, D.A. Tomalia, J.R. Baker, Langmuir 17 (2001) 2768.
[64] T. Müller, D.G. Yablon, R. Karchner, D. Knapp, M.H. Kleinman, H. Fang, C.J. Durning, D.A. Tomalia, N.J. Turro, G.W. Flynn, Langmuir 18 (2002) 7452.
[65] R. Pecora, Basic concepts – scattering and time correlation functions, in: R. Borsali, R. Pecora (Editors), Soft Matter Characterization, Springer-Verlag, Berlin, Germany, 2008, p. 2.
[66] G.H. Michler, Electron microscopy of polymers, in: H. Pash (Editor), Springer Laboratory Series, Springer, Berlin Germany, 2008.
[67] D.B. Williams, C.B. Carter, Scattering and diffraction, in: Transmission Electron Microscopy, Springer US, New York, USA, 2009, p. 23.
[68] B. Chu, Dynamic light scattering, in: R. Borsali, R. Pecora (Editors), Soft Matter Characterization, Springer-Verlag, Berlin, Germany, 2008, p. 335.
[69] B.J. Bauer, E.J. Amis, Characterization of dendritically branched polymers by small angle neutron scattering (SANS), small angle X-ray scattering (SAXS) and transmission electron microscopy (TEM), in: J.M.J. Fréchet, D.A. Tomalia (Editors), Dendrimers and Other Dendritic Polymers, John Wiley & Son, Chichester, West Sussex, UK, 2001, p. 255.
[70] T.J. Prosa, B.J. Bauer, E.J. Amis, Macromolecules 34 (2001) 4897.
[71] J. Subbi, R. Aguraiuja, R. Tanner, V. Allikmaa, M. Lopp, Eur. Polym. J. 41 (2005) 2552.
[72] S. Lee, H. Kwen, S. Lee, S. Nehete, Anal. Bioanal. Chem. 396 (2010) 1581.
[73] L.D. Hicks, J.-R. Alattia, M. Ikura, C.M. Kay, Multiangle laser light scattering and sedimentation equilibrium, in: H.J. Volgel (Editor), Calcium-Binding Protein Protocols. Volume II: Methods and Techniques, Humana Press, Totowa, New Jersey, USA, 2002, p. 127.
[74] C.A. Cason, S.A. Oehrle, T.A. Fabre, C.D. Girten, K.A. Walters, D.A. Tomalia, K.L. Haik, H.A. Bullen, J. Nanomat. (2008) Article ID 456082.
[75] J.R. Lead, K.J. Wilkinson, Environ. Chem. 3 (2006) 159.
[76] X. Shi, X. Bi, T.R. Ganser, S. Hong, L.A. Myc, A. Desai, M.M.B. Holl, J.R. Baker Jr., Analyst (Cambridge, UK) 131 (2006) 842.
[77] M.T. Islam, I.J. Majoros, J.J.R. Baker, J. Chromatogr., B 822 (2005) 21.
[78] F.R. Phelan Jr., B.J. Bauer, Chem. Eng. Sci. 62 (2007) 4620.
[79] F.v.d. Kammer, M. Baborowski, K. Friese, Anal. Chim. Acta 552 (2005) 166.
[80] I.J. Majoros, C.R. Williams, D.A. Tomalia, J.R. Baker, Macromolecules 41 (2008) 8372.
[81] Internal communication.
[82] R. Müller, C. Laschober, W.W. Szymanski, G. Allmaier, Macromolecules 40 (2007) 5599.
[83] J. Peterson, V. Allikmaa, J. Subbi, T. Pehk, M. Lopp, Eur. Polym. J. 39 (2003) 33.
[84] R. Duncan, L. Izzo, Adv. Drug Delivery Rev. 57 (2005) 2215.
[85] T.C.K. Heiden, E. Dengler, W.J. Kao, W. Heideman, R.E. Peterson, Toxicol. Appl. Pharmacol. 225 (2007) 70.
[86] M. Mortimer, K. Kasemets, M. Heinlaan, I. Kurvet, A. Kahru, Toxicol. In Vitro 22 (2008) 1412.
[87] P.C. Naha, M. Davoren, A. Casey, H.J. Byrne, Environ. Sci. Technol. 43 (2009) 6864.
[88] A.-N. Petit, P. Eullaffroy, T. Debenest, F. Gagné, Aquat. Toxicol. 100 (2010) 187.
[89] P.C. Naha, A. Casey, T. Tenuta, I. Lynch, K.A. Dawson, H.J. Byrne, M. Davoren, Aquat. Toxicol. 92 (2009) 146.
[90] S.P. Mukherjee, M. Davoren, H.J. Byrne, Toxicol. In Vitro 24 (2010) 169.
[91] United States Environmental Protection Agency (USEPA), Methods for measuring the acute toxicity of effluent and receiving waters to freshwater and marine organisms, Fifth Edition, EPA-821-R-02-012, USEPA, Washington, DC, USA, 2002.
[92] D.R. Fox, Australasian J. Ecotoxicol. 14 (2008) 7.